Published in final edited form as:
Stem Cells. 2009 August ; 27(8): 1887–1898. doi:10.1002/stem.103.

Regenerative Effects of Transplanted Mesenchymal Stem Cells in Fracture Healing

Froilán Granero-Moltó[1], **Jared A. Weis**[1], **Michael I. Miga**[2], **Benjamin Landis**[3], **Timothy J. Myers**[1], **Lynda O'Rear**[3], **Lara Longobardi**[1], **E. Duco Jansen**[2], **Douglas P. Mortlock**[4], and **Anna Spagnoli**[1,5,*]

[1]Department of Pediatrics, University of North Carolina at Chapel Hill, Chapel Hill, NC 27599, USA

[2]Department of Biomedical Engineering, Vanderbilt University Nashville, TN, 37232, USA

[3]Department of Pediatrics, Vanderbilt University Nashville, TN, 37232, USA

[4]Department of Molecular Physiology and Biophysics, Vanderbilt University Nashville, TN, 37232, USA

[5]Department of Biomedical Engineering, University of North Carolina at Chapel Hill, Chapel Hill, NC, 27599, USA

Abstract

Mesenchymal stem cells (MSC) have a therapeutic potential in patients with fractures to reduce the time of healing and treat non-unions. The use of MSC to treat fractures is attractive as it would be implementing a reparative process that should be in place but occurs to be defective or protracted and MSC effects would be needed only for the repairing time that is relatively brief. However, an integrated approach to define the multiple regenerative contributions of MSC to the fracture repair process is necessary before clinical trials are initiated. In this study, using a stabilized tibia fracture mouse model, we determined the dynamic migration of transplanted MSC to the fracture site, their contributions to the repair process initiation and their role in modulating the injury-related inflammatory responses. Using MSC expressing luciferase, we determined by bioluminescence imaging that the MSC migration at the fracture site is time- and dose-dependent and, it is exclusively CXCR4-dependent. MSC improved the fracture healing affecting the callus biomechanical properties and such improvement correlated with an increase in cartilage and bone content, and changes in callus morphology as determined by micro-computed-tomography and histological studies. Transplanting CMV-Cre-R26R-LacZ-MSC, we found that MSC engrafted within the callus endosteal niche. Using MSC from *BMP-2-Lac-Z* mice genetically modified using a bacterial artificial chromosome system to be β-gal reporters for BMP-2 expression, we found that MSC contributed to the callus initiation by expressing BMP-2. The knowledge of the multiple

*Author for correspondence: Anna Spagnoli, Department of Pediatrics, Division of Pediatric Endocrinology, 3341 Mason Farm Road, Campus Box: 7039, University of North Carolina at Chapel Hill, Chapel Hill, NC, 27599-7039, USA. Phone: (919) 843-6904; Fax: (919) 843-6905; spagnoa@med.unc.edu.

The authors have no conflicting financial interests.

Author contributions: Froilán Granero-Moltó: conception and design, collection and/or assembly of data, data analysis and interpretation, manuscript writing, final approval of manuscript; Jared A. Weis: conception and design; collection of data, data analysis and interpretation, final approval of manuscript; Michael I. Miga: data analysis, provision of study material, final approval of manuscript; Benjamin Landis: collection of data, data analysis, final approval of manuscript; Timothy J. Myers: collection of data, final approval of manuscript; Lynda O'Rear: collection of data, final approval of manuscript; Lara Longobardi: collection of data, final approval of manuscript; E. Duco Jansen: provision of study material, final approval of manuscript; Douglas P. Mortlock: provision of study material, final approval of manuscript; Anna Spagnoli: conception and design, financial support, collection and/or assembly of data, data analysis and interpretation, manuscript writing, final approval of manuscript.

MSC regenerative abilities in fracture healing will allow to design novel MSC-based therapies to treat fractures.

Keywords

Mesenchymal stem cells; Fracture healing; CXCR4; BMP-2; Stem cell niche

INTRODUCTION

High energy tibia fractures are threatening injuries with slow healing times averaging 43–49 weeks [1]. Furthermore, the fracture healing process is impaired in 10–20% of the fractures, resulting in non-unions and causing severe disabilities [2–4]. Non-unions are mostly treated with bone autografts that are associated with morbidities related to the harvesting procedure, have a limited supply and unpredictable repairing potential [5]. There is a compelling need to develop novel therapies to improve the fracture healing course and to treat non-unions. Mesenchymal stem cells (MSC) initiate the fracture repair process leading to the formation of a cartilaginous template (callus) that is then replaced by new bone that repairs the gap [6]. Limitation in MSC number and/or functions are hypothesized to play a critical in the pathogenesis of non-unions. MSC are present in several adult tissues including bone marrow (BM) and are capable of differentiating *in vitro* into mesenchyme cell types including chondrocytes and osteocytes while such differentiation has not been unequivocally shown *in vivo* [7]. Furthermore, both BM-MSC and BM mononuclear cells have been reported to exert beneficial effects in the healing of a limited number of patients with non-unions [8–13]. Although promising, these clinical studies are anecdotal. Before controlled clinical trials can begin, critical animal studies are necessary to determine how MSC are recruited and survive at the fracture site, their repair effectiveness and the mechanisms through which they exert their actions.

Although MSC seem to migrate into damaged tissues, their dynamic trafficking and tissue homing when systemically infused is a poorly understood process [14–16]. *Post-mortem* microscopy is the standard method to detect transplanted MSC within the tissues; however, it does not allow to study either the cell trafficking or to perform longitudinal observations and it is not quantitative. Small-animal *in vivo* imaging bioluminescence (BLI) permits to determine a semi-quantitative temporal and spatial analysis and bio-distribution of the light signal of luciferase-tagged cells within a living animal. Among chemokines and their receptors, CXCR-4 has been found to be critical in hematopoietic stem cell homing and cancer cell metastasis [17]. The CXCR4 expression and contribution to MSC migration *in vitro* and its need in MSC homing *in vivo* has been scarcely evaluated [18, 19].

Several reports have shown that MSC delivered to an injured tissue can improve the recovery; however, a limited number of MSC have been demonstrated to differentiate into the repaired tissue [20–22]. This discrepancy might be explained by the fact that: 1) there are technical difficulties in identifying MSC within the repaired tissue; 2) studies have focused on the identification of MSC differentiation into cells involved in advanced stages of healing; 3) MSC mechanisms of action, other than differentiation, may have induced the regeneration. Anti-inflammatory paracrine effects of MSC have been reported in animal models of acute and chronic inflammatory diseases [23–26]. Most recently, MSC transplant in 55 patients with severe graft-versus-host disease has led to a complete response or improvement in 39 patients [27]. It is plausible that due to their intrinsic multipotentiality, MSC have several and distinct reparative actions. Uncontrolled inflammation plays a critical role in the pathogenesis of non-unions and a selective modulation of the inflammatory response may become the target of new therapies to enhance the bone repair and to prevent

the occurrence of a non-union. The role of MSC in the initiation of the callus formation has been scarcely investigated and most of the studies have focused on more advanced repair stages either during the cartilageneous callus maturation or the mineralization process [28, 29].

Our studies were designed to determine: 1) the *in vivo* trafficking and homing within the fractured tibia of systemically transplanted MSC; 2) the need of CXCR4 for MSC homing; 3) the effects of MSC transplant in the callus biomechanical properties; 4) the MSC engraftment into the repairing tissue and contribution to the callus initiation; 5) the systemic and local anti-inflammatory effects of MSC in fracture repair.

MATERIALS AND METHODS

Reagents

7-Amino-actinomycin D (7-DAA) was from Molecular-Probes; D-luciferin from Biosynth-International.

Antibodies

Biotin-conjugated anti-mouse CD34, CD45, CD11b and CXCR4 antibodies from BD-Biosciences. Phycoerythrin-conjugated anti-mouse CXCR4, CD29, CD44, CD73, CD105, CD45 and control isotype antibodies from eBioscience.

Stabilized fracture model

All animal procedures were approved by the animal care committee of the University of North Carolina-Chapel Hill and Vanderbilt University. Stabilized tibia fractures were produced in 8–12 weeks old FVB female syngenic mice (FVB-NJ, Jackson-Laboratories) by intramedullar fixation using a 0.25mm stainless steel pin (Fine-Science-Tools) inserted through the patellar tendon inside the medullar canal of the tibia followed by closed fracture using a three-point bending device with a standardized force [30]. For pain control, bupremorphine (0.5 mg/kg) was administered subcutaneously.

Isolation and expansion of MSC

Primary cultures of BM-MSC were obtained by flushing the BM from femurs and tibias of 4–6 weeks old FVB-NJ mice as previously reported [31]. Briefly, BM nucleated plastic-adhering cells were expanded for 7–10 days without passaging [31]. Immediately before transplant, contaminating hematopoietic cells were eliminated by immunodepletion of the CD45, CD11b and CD34 positive cells using a MACS system (Miltenyi-Biotech). As shown in Supplemental Fig. 1, using this protocol we obtain a MSC population in which >90% of cells express the specific MSC markers CD73, CD29, CD44, and 67.5% the CD105 marker. Furthermore, MSC after immunodepletion were negative for CD45 (0.9±0.5%, n=3) and CD11b (1.1±1.3%, n=3). For BLI imaging, MSC were isolated from FVB/N animals constitutively expressing *Firefly luciferase* under the β-actin promoter (FVB/N-Tg(*β-Actin-luc*)-Xen) (Caliper-Life-Sciences). After fracture, mice were transplanted with 10^6 MSC by tail vein injection, unless specified. MSC were also isolated from the BM of the *CMV-R26R* or *BMP-2-Lac-Z* mice and transplanted into wild-type female littermates. The *BMP-2-Lac-Z and CMV-R26R* mice were generated as described in the Online Supplemental Materials or previously reported [32].

BLI analyses

BLI imaging was performed using an IVIS 200 imaging system (Caliper-Life-Sciences). All images were collected 15 minute after D-luciferin (150 mg/kg) intraperitoneal injection. Additional information on the BLI analyses are available in the Online Supplemental

Materials. BLI signaling at the fracture tibia site region of interest (ROI), measured as integrated photons/sec/cm^2/sr, was normalized by subtracting the background signal found in an equal ROI in the contralateral intact tibia. Imaging data were analyzed using the LivingImages2.20.1 (Xenogen-Corp.).

Luciferase expressing adenoviruses and MSC infection

An adenoviral vector that encodes the *Firefly luciferase* under the control of a cytomegalovirus promoter was used to generate highly purified (CsCl gradient) viruses as previously described [33]. All the experiments were performed using a multiplicity of infection of 1,000 in MSC cultured for 7 days. Additional information are provided in the Online Supplemental Materials.

Biomechanical testing (BMT)

Fractured tibias were dissected 14 days post-fracture, wrapped PBS-embedded gauze and stored at −80°C until analysis. The bone ends were embedded with polymethylmetacrylate and loaded into the electroforce-based system ELF 3100 (Bose). The displacement rate was at 0.25 mm/min and a force-displacement curve recorded to calculate the ultimate distraction (maximum distraction at failure), ultimate force (maximum force at failure), toughness (area under the curve) and stiffness (maximum slope) using the WinTestControl Software (Bose).

Histology and *in situ* hybridization

Tibias were dissected 7 and 14 days post-fracture, histologically prepared and the entire callus sectioned (6μm). The callus center was identified as the largest diameter by H&E staining and analyses performed within 20 sections from the center. *In situ* hybridization analysis was performed as previously reported [34]. Plasmid with insertion of mouse Collagen (II)-alpha1-chain (*Col2a1*) was provided by D. Kingsley (Stanford University), mouse Collagen (I)-alpha-1-chain (*Col1a1*) and mouse *Osteocalcin* by G. Karsenty (Columbia University),. Probe for mouse Collagen (X)alpha1chain (*Col10a1*) was generated as previously described [35]. Images were taken using an Olympus BX51 microscope with a DP71 camera, imported into Adobe Photoshop and formatted without using any imaging enhancement.

Micro computed tomography μCT) analysis of fracture calluses

Tibia fractures were dissected 14 days post-fracture, and following removal of the pin and μCT scanned (Scanco Medical 3CT40). μCT imaging were obtained at 55 kVp, 145 μA, 300 ms integration time using 63m voxel resolution along 5.2 mm length centered at the fracture line with a total scanning time of approximately 1 hour[36]. To determine material type from μCT scans, a parametric thresholding study was performed by serial μCT scanning and histological analysis as reported in the Online Supplemental Materials.

Circulating and callus cytokine measurements

Sera were obtained from mice that received MSC transplant and controls at day 1, 3 and 7 post-fracture. Tumor necrosis factor-α (TNF-α), interleukin-1 β (IL-1β), interleukin-10 (IL-10), interleukin-13 (IL-13), interleukin-6 (IL-6) levels were determined using LINCOplex immunoassay (LINCO-Research). Total RNA obtained using Trizol and PureLinK columns (Invitrogen) from dissected calluses 3 and 7 days after fracture was reversed transcribed using SuperScript III reverse transcriptase (Invitrogen) and Oligod(T)16 (Applied Biosystems). *TNF-α* mRNA expression was measured by qRT-PCR (MyIQ-Single-Color-RT-PCR-System, Biorad) using Syber Green as previously described [37]. PCR primers for *TNF-α* amplification were: 5′-CCACCACGCTCTTCTGTCTAC-3′ and 5′-GGCTACAGGCTTGTCACTCG-3′. Samples

were run in triplicates, data were normalized to β-actin expression and analyzed using the $2^{-\Delta\Delta CT}$ method and expressed as fold of increases compared with the average of an untransplanted control, which was given the value of 1.

X-Gal staining

X-Gal staining was performed as previously described with some modifications [32]. Briefly, the fractured tibia was dissected, briefly fixed with 0.4% PFA and stained at room temperature with X-Gal staining solution. To achieve specific localization of cells which express prokaryotic (*Escherichia coli*) β-galactosidase, pH of the reacting solution was adjusted to selectively favor its activity over that of the mammalian enzyme [38, 39]. After staining, samples were fixed with 4% PFA for 24h paraffin embedded and sections were counter-stained using nuclear fast red as previously described [32, 35]. CMV-R26R-LacZ-MSC (1×10^5) were placed in 10μl medium in a 24-well plate and after 1 hour, 500μl of medium was added; cells were cultured for 24 hours and X-Gal stained as previously reported [35].

Statistics

Data are expressed as mean ± SD. Statistical analyses were performed using unpaired Student's *t*-test, ANOVA followed by *post-hoc* multiple comparison testing. the relationship between number of transplanted MSC and BLI signal was analyzed using a dose-response sigmoid curve. The Graph-pad Prism Software was used. Statistical significance was set at $p<0.05$.

Online supplemental materials

Online supplemental material is available.

RESULTS

Systemically transplanted MSC: in vivo dynamic and time-dependent recruitment at the fracture site

To assess the *in vivo* MSC dynamic trafficking and homing in response to a pathological tibia fracture cue, 1×10^6 MSC-β-Act-Luc, constitutively expressing *luciferase*, were transplanted into a mouse with stabilized tibia fracture and sequential BLI imaging was performed from day 1 to day 14 post-fracture/transplant. As depicted in Fig. 1A (left panel), one day after the fracture/transplant MSC-β-Act-Luc were visualized at the lung site. On day 3 after the fracture, we observed that MSC began to localize at the fractured leg site (right tibia) where they persisted up to 14 days after the fracture/transplant (Fig. 1A, left panel). Semi-quantitative analysis of the BLI signal of luciferase-tagged MSC over the fractured leg, was time-dependent, increasing progressively from day 1 to day 7, without any further increase at day 14.

The presence of CXCR4 is essential for MSC homing at the fracture site

The finding that MSC have the ability to migrate to an injured tibia implies that they own specific homing signal(s). While CXCR4 has been involved in the hematopoietic stem cell engraftment and cancer cell metastasis, its role in MSC homing still needs to be defined [18, 19, 40–42]. In our study, using primary cultures of unpassaged MSC immunodepleted of hematopoietic cells, we first found that ~30% of MSC express CXCR4 (34.2±4.7%, n=4 MSC cultures obtained from the BM of at least 4 mice for each culture). Second, we separated, using CXCR4 immunoselection, the MSC population as MSC-CXCR4(+) and MSC-CXCR4(−) populations that were injected into a mouse with a tibia fracture. One day post-fracture both MSC-CXCR4(+) and MSC-CXCR4(−) had a

localization pattern similar to the unselected MSC (Fig. 1A). However, at day 3, MSC-CXCR(−) were not capable of homing to the fracture site, while the MSC-CXCR(+) showed an intense signal (Fig. 1A, middle and right panels). A similar scenario was observed at day 7 and day 14 following the fracture/transplant (Fig. 1, middle and right panels). As shown in Fig. 1B, semi-quantitative analysis of the BLI signal confirmed that the MSC-CXCR4(−) migration to the fracture site at any studied time-point was negligible; whereas, MSC-CXCR4(+) showed a time-dependent increase of MSC-luciferase signal at the fractured tibia. Our data demonstrate that systemically transplanted MSC are capable of homing at the fracture site and the migration is dependent on the presence of CXCR4.

Dose-dependent MSC homing at the fracture site

To assess the dose-dependent MSC homing at the fracture site, we systemically infused MSC transduced with an adenoviral vector expressing *luciferase* (MSC-Adn-Luc) into mice with a tibia fracture. We reasoned that since adenoviruses do not integrate in the host genome, and expression is lost in dividing cells, the luciferase signal would exclusively assess the MSC migration to the fracture site. As shown in Supplemental Fig. 3A, in mice with fractured tibia transplanted with increasing doses of MSC-Adn-Luc (from 5×10^3 to 1000×10^3 MSC) and BLI imaged 3 days later, we found that MSC homing was dose-dependent. Interestingly, we found the ED_{50} to be a dose of 300×103, with a plateau at 700×103 without any significant increase at a dose of 1000×10^3 (Supplemental Fig. 3C). This finding indicates that MSC migration to the injured site reaches a saturation point and a limiting mechanism that needs further investigations can be hypothesized.

MSC improve the biomechanical properties of the fracture callus

A critical feature of bone healing is that the regenerated tissue provides sufficient strength to the injured limb in order to regain function. To investigate whether MSC improved the callus material properties we performed distraction-to-failure BMT. Dissected calluses from MSC recipient mice (MSC) as well as control calluses from mice that did not receive MSC (no cells), were subjected to a gradual distraction force until they broke. As shown in Table 1, calluses of mice that received MSC had increased toughness and ultimate displacement compared to controls. The peak force was not different in the two groups while, there was a trend over a decrease of callus stiffness in the mice that received MSC. Taken together, these data indicate that MSC improved the callus material properties making the tissue less brittle by decreasing the structural rigidity.

MSC effects on callus size and morphology

To determine material type (bone and soft tissue) from μCT scans, a parametric threshold study of an entire callus was performed by serial μCT scanning and histological analyses (*in situ* hybridizations for *Collagen 1*, *Collagen 10*, and Trichrome-Blue and Safranin-O/Fast-Green staining) (see Supplemental Materials). Mice that received MSC transplant displayed a significant increase of the total volume, as well as total bone, soft tissue, new bone, and callus volumes and callus mineralization content compared to controls (Fig. 2A). The three-dimensional reconstructions of the entire calluses as well as the sagittal sections showed remarkable differences in the size and morphology of the new mineralized callus in mice that received MSC *versus* controls. As shown in Fig. 2B, the most notable differences were that: 1) a large callus surrounded the fractured bone edges as well as the intact cortical bone in the calluses from mice transplanted with MSC, but remained limited to the ends of the bone segments in the controls [compare panels B1 with B5 and B3 with B7]; 2) a continuous net of the creeping callus bridging the fracture gap in MSC recipient mice versus the limited connectivity observed in the controls [compare panels B2 with B6 and B4 with B8]. These findings indicate that MSC transplant by providing a more organized bridge between the bone ends improves the repairing process and therefore its material properties.

MSC effects on callus histology

We next analyzed the callus histology as well as bone and cartilaginous marker expressions at day 7 and 14 after the fracture and MSC transplant. H&E staining analyses, showed that at 7-days, the calluses from mice transplanted with MSC were bigger than controls and demonstrated larger areas of cartilage-like tissue (Fig. 3A). *In situ* hybridization for *Collagen 2* and *Collagen 10* expression as well as Safranin-O staining revealed a more abundant presence of either chondrocytes or hypertrophic chondrocytes in the calluses from mice transplanted with MSC, indicating that the fracture repair in those mice more predominately proceeded through an endochondral ossification process than controls (Fig. 3A). When evaluated at 14 days after the fracture, *Collagen 10* expression was also consistently higher in mice that received MSC than controls and at this time, it was associated with an increase of *Collagen 1* expression indicating that the endochondral callus progressed to bone formation (Fig. 3B).

MSC distribution within the callus

To analyze the cellular distribution of transplanted MSC within the callus, fractured mice were transplanted with MSC from *CMV-R26R* mice and 7 days after fracture-transplant dissected calluses were Lac-Z stained. As shown in Supplemental Fig. 4, CMV-R26R-LacZ-MSC express stainable β-Gal activity, indicating this as a suitable reporter system for MSC. As negative control for the Lac-Z staining protocol, 7-day post fracture calluses from wild-type mice were Lac-Z stained. As shown in the Supplemental Fig. 5, no staining was detectable indicating that the protocol used did not result in any background.

As shown in Fig. 4A, we found that transplanted CMV-R26R-LacZ-MSC localized within specific areas of the callus, in particular within the fracture ridge, the endosteum close to the fracture rim and the BM. Counterstaining the calluses with Safranin-O/Fast-Green (Fig. 5B), we identified that MSC localized within the endosteal callus in the areas of most active bone formation. Higher magnification of these areas showed that the Lac-z positive MSC (stained in Blue) were embedded in the bone matrix (stained in Green) as osteoblasts within the newly forming bone (Fig. 5C) or as newly formed osteocytes with abundant cytoplasm (Fig. 5D). As shown in Supplemental Fig. 6, *in situ* hybridization analysis confirmed that within the margins of the woven bone, some of the Lac-z positive MSC expressed also *osteocalcin* confirming their ability to differentiate into osteoblasts. Our findings indicate that transplanted MSC localize within different and specific niches of the callus and the number of MSC within the newly forming bone seems to be limited compared to the significant effects of MSC on the callus biomechanical properties. This observation led us to hypothesize that the contributions of MSC to the fracture healing is likely through multiple mechanisms that include but cannot limited to the callus mineralization.

MSC contribute to the callus initiation by expressing BMP-2

To determine the contribution of MSC to the initial phase of the callus formation, we analyzed whether transplanted MSC were capable of expressing BMP-2 within the callus. BMP-2 is highly expressed during fracture healing and is essential for the callus initiation [43]. In fact, in mice null for BMP-2 expression in limb mesenchyme progenitors, the earliest steps of fracture healing are blocked and mice lack fracture healing [43]. For this purpose, we obtained MSC from *BMP-2-Lac-Z* mice genetically modified using a BAC system to be β-gal reporters for BMP-2 expression [32]. BMP-2-Lac-Z–MSC were transplanted into fractured mice, calluses were dissected 7 days after the fracture and Lac-Z stained. We found that BMP-2-Lac-Z-MSC localized within the fracture rim and more peculiarly along the endosteum adjacent to the fracture edges (Fig. 5A–B). This pattern was similar to the pattern observed in the fractured mice transplanted with CMV-R26R-LacZ-MSC, although the mice transplanted with BMP-2-Lac-Z–MSC lacked the Lac-Z staining

within the BM cells. Our data indicate that transplanted MSC localize at the fracture site and are capable of expressing BMP-2, an essential gene for initiating the fracture repair process. To determine the endogenous BMP-2 expression at the same fracture healing stage, calluses were obtained 7 days after fracture from *BMP-2-Lac-Z* fractured mice and Lac-Z stained. As shown in Fig 5C–D, we found that BMP-2 is highly expressed at the fracture rim and interestingly no expression was detectable at the endosteal site. This observation may indicate that the endosteum is a peculiar niche where the transplanted MSC engraft and express BMP-2.

MSC transplant modulates the systemic and local inflammatory responses

To determine whether the beneficial contributions of MSC to the fracture healing was associated with an anti-inflammatory action, we sequentially determined the circulating levels of a set of cytokines in the serum of mice either transplanted with MSC or controls. As shown in Fig. 6, over the first week after the fracture, MSC transplant selectively down-regulated the serum levels of TNF-α and IL-1β abolishing the injury-induced inflammatory response found in the control fractured mice. The MSC anti-inflammatory action was targeted to specific cytokines, in fact, MSC had no effect on IL-13 and IL-10 at any time and had only a significant effect reducing IL-6 levels at day 3 post-fracture (Fig. 6C–E). MSC had similar effects on the local mRNA expression of TNF-α that was decreased in the calluses from MSC transplanted mice compared to controls at day 3 (MSC: 1.278±1.741 fold of change; control: 3.78±3.006; $P<0.05$; n=6) and day 7 (MSC: 0.670±0.315 fold of change; control: 2.729±2.334; $P<0.05$; n=6) post-fracture.

DISCUSSION

In our studies, we have characterized, in living animals, the dynamic migration of MSC in response to a bone fracture and determined that this specific migration at the site of injury is driven by CXCR4. We have also demonstrated that MSC transplant induces a biomechanical improvement of the healing process that is associated with an increase in the callus volumes and cartilageneous and bone contents. We have found that MSC engraft into specific niches of the callus expressing the fracture repair initiator BMP-2 and that the delivery of MSC has a specific systemic and local anti-inflammatory effect. In summary, our report provides a comprehensive assessment of the contributions of transplanted MSC to the fracture healing process.

There is a significant body of evidence that links MSC to tissue regeneration, including bone and cartilage [20]. However, *in vivo* studies have been primarily performed using *post-mortem* analyses; as a result longitudinal evaluations of MSC dynamic in living animals are scarce [15]. Furthermore, studies have been limited in the attempt to demonstrate one of the regenerative effects of MSC, mostly the differentiation into bone, lacking an ample evaluation of the multiple actions of MSC. The regeneration of damaged tissue implies that different responses converge at the damaged area. The regenerative cells need to be recruited at the injury site, control the injury-induced responses and eventually contribute to the repair. In our studies, we have demonstrated that MSC exert their regenerative properties by contributing to each of the stages of fracture healing. Transplanting MSC tagged with luciferase in combination with BLI analysis, we have demonstrated that MSC migrate to a fracture site and migration is time- and dose-dependent. Recruitment of circulating progenitor cells to the site of injury occurs as a normal biological process during the fracture process [44]. We hypothesize that MSC injected systemically migrate to the fracture site using a similar injury-related recruitment mechanism. Gao et al, using ^{111}I-indium-MSC investigated the MSC dynamic only for 48 hours after cell infusion into normal non-injured rats [15]. Authors found that after injection, cells distributed into the lungs and the liver and a vasodilator increased the liver localization [15]. We found similar results in our short-term

BLI studies, but our long-term analyses in fractured mice allowed us to determine that three days after the fracture/transplant, MSC were specifically recruited at the fracture site where they remained up to 14 days. Thus, the use of MSC transplant seems to be a valid strategy to allow a non-invasive increase of viable progenitors at a fracture site.

We have found that fracture MSC migration is dependent on the presence of CXCR4. There are discordant data on whether MSC express CXCR4 and its role in MSC migration [18, 19, 40–42]. Differences in culture passages may be the reason for such discordances; in fact, cell passaging causes a down-regulation of CXCR4 expression and loss of MSC homing [18, 45, 46]. We have used primary cultures of unpassaged MSC immunodepleted of hematopoietic cells and found a consistent CXCR4 expression in ~30% of the MSC population. Cheng *et al.*, have recently reported that MSC recruitment was enhanced in a rat model of myocardial infarction by retrovirally overexpressing CXCR-4 in MSC that lacked CXCR4[47]. In our study, we have found that, without any CXCR-4 manipulation, native primary cultured MSC are capable of homing at a fracture site in a CXCR4 dependent manner.

In our study, we found that MSC transplant improves the fracture healing by increasing the material toughness of the callus and causing it to be less brittle. The observed biomechanical material data were consistent with the μCT imaging that showed in MSC recipient mice some remarkable differences in the callus geometry that was larger with more organized bridging structures characterized by soft tissue and new bone. Histological analyses confirmed that the fracture healing in MSC recipient mice progressed through more cartilage and newly mineralized bone than controls. Tibia fractures necessitate long period for healing. Optimization of clinical management can reduce the healing time, however it has been pointed out that even if osteogenic cells at the fracture site are working at full capacity, they will not heal the defect if too few cells are present, nor will any drug, directed at enhancing bone formation be effective since maximal osteogenesis per cell is already occurring [48]. Our studies provide evidence that even in a normal fracture healing tibia model, MSC transplant enhances the repair process supporting the use of MSC to provide a critical number of regenerative cells to achieve the desired bone-repairing results in patients with high-energy fractures. Although some non-union animal models are available, these models are based either on mice with genetic defects that lead to repair impairments, or by creating large bone gaps or stripping the periosteum in order to decrease the number of regenerative progenitors. None of these models reflects the mechanisms for non-unions found in patients. Furthermore, the healing times in those models are largely inconsistent making problematic the interpretation of results when multiple experimental groups are studied. On the other hand, the stabilized fracture tibia model we have used has a consistent healing time and having found that in this model, MSC have several positive effects opens optimistic prospective for using MSC in non-unions.

In our studies using Lac-Z tagged MSC, we found that transplanted MSC localize along the margins of woven bone where they assume the morphology of active osteoblasts, express osteocalcin and associate with the endosteal surface. Interestingly, MSC did not localize within the periosteal callus although the overall size of the callus of MSC transplanted mice was larger and showed larger areas of newly forming bone. This observation led us to pursue studies aimed at determining whether the MSC regenerative effects were not exclusively related to their differentiative abilities into bone but also to their contributions on the initiation of the healing process. Our study is the first to report that systemically injected MSC localize at the fracture site where they are capable of expressing BMP-2, an essential initiator of the fracture repair process [43]. One interesting finding from our study is that MSC expressing BMP-2 localize very distinctly at the endosteum site. The endosteum maintains the bone homeostasis, participates in the fracture healing process and a lack of the

endosteal callus formation is critical in the pathogenesis of non-unions [49–51]. Several cells form the endosteal niche including osteoblasts, CXCL12-abundant reticular (CAR) cells, MSC and hematopoietic stem cells. There is a large body of evidence that support the notion that the endosteal osteoblasts provide a variety of factors that regulate the hematopoietic stem cell number and function [reviewed in [52, 53]]. It has been hypothesized that in the endosteal niche CAR cells together osteoblasts, and potentially other cell types, generate a hypoxic environment that maintains the hematopoietic stem cells in a quiescent state [53]. The inhibitory effect of MSC on cell proliferation *in vitro* raises the possibility of a MSC role in maintaining the hematopoietic stem cells in this quiescent state [54]. On the other hand, hemapotopoietic stem cells regulate MSC induction into osteoblasts *in vitro* as well as *ex-vivo* [55]. Our knowledge of the MSC niches within native tissues is very poor and even less is known about the MSC niches after transplant. Our study provides evidence for the homing of circulating transplanted MSC in response to a fracture injury cue into the endosteal niche, where they express BMP-2. It is plausible that MSC expressing CXCR4 are recruited to the endosteal niche by CAR cells. We hypothesize that MSC within the endosteal niche can either differentiate into osteoblasts, or through a paracrine action, control the injury-related inflammatory response. It will be of great interest to evaluate in future longitudinal studies the contributions of MSC through all the reparative process.

Several studies have shown that MSC have the ability to suppress the inflammatory response *in vitro* as well as *in vivo* (reviewed in [20, 22]). These anti-inflammatory effects were induced through paracrine mechanisms that shifted the tissue milieu from a pro-inflammatory to an anti-inflammatory state [23–26]. During the tissue repairing process a precise temporal and spatial resolution of the inflammatory response is critical to limit the tissue injury, to prevent the development of fibrosis, and ultimately to promote the regeneration. Uncontrolled inflammation plays a critical role in the pathogenesis of non-unions. Traditional anti-inflammatory drugs that block the cytokine response *in toto* are unable to direct and selectively control the process and may actually have negative effects on the healing process. In our study, we have found that the beneficial effects of MSC transplant on fracture regeneration are associated with a selective effect on systemic and local cytokine production. MSC as selective modulators of the inflammatory response may become the target of new therapies to enhance the healing process in patients with non-unions.

Supplementary Material

Refer to Web version on PubMed Central for supplementary material.

Acknowledgments

This work was supported by a National Institutes of Health Grant 5R01DK070929-02 (to A.S.). We acknowledge the support of the Vanderbilt Emphasis Program and the Endocrine Society Summer Research Fellowships (to B.L.). We recognize the technical support of the Biomedical Research Imaging Center at University of North Carolina at Chapel Hill, the Vanderbilt Institute of Imaging Science and the Vanderbilt's Institutional Immunohistochemistry Core at Vanderbilt University. We thank K. Shimer for her early participation to the BLI analyses. We acknowledge Ron Chandler for his technical advice. We thank D. Kingsley and G. Karsenty for providing reagents.

References

1. Keating JF, Blachut PA, O'Brien PJ, et al. Reamed nailing of Gustilo grade-IIIB tibial fractures. The Journal of bone and joint surgery. 2000; 82:1113–1116. [PubMed: 11132268]
2. Einhorn TA. Enhancement of fracture-healing. J Bone Joint Surg Am. 1995; 77:940–956. [PubMed: 7782368]
3. Marsh D. Concepts of fracture union, delayed union, and nonunion. Clin Orthop. 1998:S22–30. [PubMed: 9917623]

4. Praemer, A.; Furner, S.; Rice, DP. Musculoskeletal Conditions in the United States. 2. Rosemont HL: The American Academy of Orthopaedic Surgeons; Park Ridge, Illinois: 1999.
5. Morshed S, Corrales L, Genant H, et al. Outcome assessment in clinical trials of fracture-healing. J Bone Joint Surg Am. 2008; 90 (Suppl 1):62–67. [PubMed: 18292359]
6. Einhorn TA. The cell and molecular biology of fracture healing. Clin Orthop Relat Res. 1998:S7–21. [PubMed: 9917622]
7. Pittenger MF, Mackay AM, Beck SC, et al. Multilineage potential of adult human mesenchymal stem cells. Science. 1999; 284:143–147. [PubMed: 10102814]
8. Marcacci M, Kon E, Moukhachev V, et al. Stem cells associated with macroporous bioceramics for long bone repair: 6- to 7-year outcome of a pilot clinical study. Tissue Eng. 2007; 13:947–955. [PubMed: 17484701]
9. Quarto R, Mastrogiacomo M, Cancedda R, et al. Repair of large bone defects with the use of autologous bone marrow stromal cells. N Engl J Med. 2001; 344:385–386. [PubMed: 11195802]
10. Hernigou P, Mathieu G, Poignard A, et al. Percutaneous autologous bone-marrow grafting for nonunions. Surgical technique. J Bone Joint Surg Am. 2006; 88(Suppl 1 Pt 2):322–327. [PubMed: 16951103]
11. Hernigou P, Poignard A, Beaujean F, et al. Percutaneous autologous bone-marrow grafting for nonunions. Influence of the number and concentration of progenitor cells. J Bone Joint Surg Am. 2005; 87:1430–1437. [PubMed: 15995108]
12. Hernigou P, Poignard A, Manicom O, et al. The use of percutaneous autologous bone marrow transplantation in nonunion and avascular necrosis of bone. J Bone Joint Surg Br. 2005; 87:896–902. [PubMed: 15972899]
13. Tseng SS, Lee MA, Reddi AH. Nonunions and the potential of stem cells in fracture-healing. J Bone Joint Surg Am. 2008; 90 (Suppl 1):92–98. [PubMed: 18292363]
14. Chapel A, Bertho JM, Bensidhoum M, et al. Mesenchymal stem cells home to injured tissues when co-infused with hematopoietic cells to treat a radiation-induced multi-organ failure syndrome. J Gene Med. 2003; 5:1028–1038. [PubMed: 14661178]
15. Gao J, Dennis JE, Muzic RF, et al. The dynamic in vivo distribution of bone marrow-derived mesenchymal stem cells after infusion. Cells Tissues Organs. 2001; 169:12–20. [PubMed: 11340257]
16. Barbash IM, Chouraqui P, Baron J, et al. Systemic delivery of bone marrow-derived mesenchymal stem cells to the infarcted myocardium: feasibility, cell migration, and body distribution. Circulation. 2003; 108:863–868. [PubMed: 12900340]
17. Zou YR, Kottmann AH, Kuroda M, et al. Function of the chemokine receptor CXCR4 in haematopoiesis and in cerebellar development. Nature. 1998; 393:595–599. [PubMed: 9634238]
18. Wynn RF, Hart CA, Corradi-Perini C, et al. A small proportion of mesenchymal stem cells strongly expresses functionally active CXCR4 receptor capable of promoting migration to bone marrow. Blood. 2004; 104:2643–2645. [PubMed: 15251986]
19. Von Luttichau I, Notohamiprodjo M, Wechselberger A, et al. Human adult CD34-progenitor cells functionally express the chemokine receptors CCR1, CCR4, CCR7, CXCR5, and CCR10 but not CXCR4. Stem Cells Dev. 2005; 14:329–336. [PubMed: 15969628]
20. Granero-Molto F, Weis JA, Longobardi L, et al. Role of mesenchymal stem cells in regenerative medicine: application to bone and cartilage repair. Expert Opin Biol Ther. 2008; 8:255–268. [PubMed: 18294098]
21. Le Blanc K, Gotherstrom C, Ringden O, et al. Fetal mesenchymal stem-cell engraftment in bone after in utero transplantation in a patient with severe osteogenesis imperfecta. Transplantation. 2005; 79:1607–1614. [PubMed: 15940052]
22. da Silva Meirelles L, Caplan AI, Nardi NB. In search of the in vivo identity of mesenchymal stem cells. Stem Cells. 2008; 26:2287–2299. [PubMed: 18566331]
23. Ortiz LA, Gambelli F, McBride C, et al. Mesenchymal stem cell engraftment in lung is enhanced in response to bleomycin exposure and ameliorates its fibrotic effects. Proc Natl Acad Sci U S A. 2003; 100:8407–8411. [PubMed: 12815096]

24. Zappia E, Casazza S, Pedemonte E, et al. Mesenchymal stem cells ameliorate experimental autoimmune encephalomyelitis inducing T-cell anergy. Blood. 2005; 106:1755–1761. [PubMed: 15905186]
25. Parekkadan B, van Poll D, Suganuma K, et al. Mesenchymal stem cell-derived molecules reverse fulminant hepatic failure. PLoS ONE. 2007; 2:e941. [PubMed: 17895982]
26. Bartholomew A, Sturgeon C, Siatskas M, et al. Mesenchymal stem cells suppress lymphocyte proliferation in vitro and prolong skin graft survival in vivo. Exp Hematol. 2002; 30:42–48. [PubMed: 11823036]
27. Le Blanc K, Frassoni F, Ball L, et al. Mesenchymal stem cells for treatment of steroid-resistant, severe, acute graft-versus-host disease: a phase II study. Lancet. 2008; 371:1579–1586. [PubMed: 18468541]
28. Bruder SP, Jaiswal N, Ricalton NS, et al. Mesenchymal stem cells in osteobiology and applied bone regeneration. Clin Orthop. 1998:S247–256. [PubMed: 9917644]
29. Petite H, Viateau V, Bensaid W, et al. Tissue-engineered bone regeneration. Nat Biotechnol. 2000; 18:959–963. [PubMed: 10973216]
30. Bonnarens F, Einhorn TA. Production of a standard closed fracture in laboratory animal bone. J Orthop Res. 1984; 2:97–101. [PubMed: 6491805]
31. Spagnoli A, Longobardi L, O'Rear L. Cartilage disorders: potential therapeutic use of mesenchymal stem cells. Endocr Dev. 2005; 9:17–30. [PubMed: 15879685]
32. Chandler RL, Chandler KJ, McFarland KA, et al. Bmp2 transcription in osteoblast progenitors is regulated by a distant 3′ enhancer located 156.3 kilobases from the promoter. Mol Cell Biol. 2007; 27:2934–2951. [PubMed: 17283059]
33. Fowler M, Virostko J, Chen Z, et al. Assessment of pancreatic islet mass after islet transplantation using in vivo bioluminescence imaging. Transplantation. 2005; 79:768–776. [PubMed: 15818318]
34. Deal KK, Cantrell VA, Chandler RL, et al. Distant regulatory elements in a Sox10-beta GEO BAC transgene are required for expression of Sox10 in the enteric nervous system and other neural crest-derived tissues. Dev Dyn. 2006; 235:1413–1432. [PubMed: 16586440]
35. Spagnoli A, O'Rear L, Chandler RL, et al. TGF-beta signaling is essential for joint morphogenesis. J Cell Biol. 2007; 177:1105–1117. [PubMed: 17576802]
36. Reynolds DG, Hock C, Shaikh S, et al. Micro-computed tomography prediction of biomechanical strength in murine structural bone grafts. J Biomech. 2007; 40:3178–3186. [PubMed: 17524409]
37. Longobardi L, O'Rear L, Aakula S, et al. Effect of IGF-I in the chondrogenesis of bone marrow mesenchymal stem cells in the presence or absence of TGF-beta signaling. J Bone Miner Res. 2006; 21:626–636. [PubMed: 16598383]
38. Nolan GP, Fiering S, Nicolas JF, et al. Fluorescence-activated cell analysis and sorting of viable mammalian cells based on beta-D-galactosidase activity after transduction of Escherichia coli lacZ. Proc Natl Acad Sci U S A. 1988; 85:2603–2607. [PubMed: 3128790]
39. Devine MJ, Mierisch CM, Jang E, et al. Transplanted bone marrow cells localize to fracture callus in a mouse model. J Orthop Res. 2002; 20:1232–1239. [PubMed: 12472234]
40. Honczarenko M, Le Y, Swierkowski M, et al. Human bone marrow stromal cells express a distinct set of biologically functional chemokine receptors. Stem Cells. 2006; 24:1030–1041. [PubMed: 16253981]
41. Chamberlain G, Wright K, Rot A, et al. Murine mesenchymal stem cells exhibit a restricted repertoire of functional chemokine receptors: comparison with human. PLoS ONE. 2008; 3:e2934. [PubMed: 18698345]
42. Fox JM, Chamberlain G, Ashton BA, et al. Recent advances into the understanding of mesenchymal stem cell trafficking. Br J Haematol. 2007; 137:491–502. [PubMed: 17539772]
43. Tsuji K, Bandyopadhyay A, Harfe BD, et al. BMP2 activity, although dispensable for bone formation, is required for the initiation of fracture healing. Nat Genet. 2006; 38:1424–1429. [PubMed: 17099713]
44. Kumagai K, Vasanji A, Drazba JA, et al. Circulating cells with osteogenic potential are physiologically mobilized into the fracture healing site in the parabiotic mice model. J Orthop Res. 2008; 26:165–175. [PubMed: 17729300]

45. Peled A, Petit I, Kollet O, et al. Dependence of human stem cell engraftment and repopulation of NOD/SCID mice on CXCR4. Science. 1999; 283:845–848. [PubMed: 9933168]

46. Rombouts WJ, Ploemacher RE. Primary murine MSC show highly efficient homing to the bone marrow but lose homing ability following culture. Leukemia. 2003; 17:160–170. [PubMed: 12529674]

47. Cheng Z, Ou L, Zhou X, et al. Targeted migration of mesenchymal stem cells modified with CXCR4 gene to infarcted myocardium improves cardiac performance. Mol Ther. 2008; 16:571–579. [PubMed: 18253156]

48. Bruder SP, Fink DJ, Caplan AI. Mesenchymal stem cells in bone development, bone repair, and skeletal regeneration therapy. Journal of cellular biochemistry. 1994; 56:283–294. [PubMed: 7876320]

49. Szulc P, Delmas PD. Bone loss in elderly men: increased endosteal bone loss and stable periosteal apposition. The prospective MINOS study. Osteoporos Int. 2007; 18:495–503. [PubMed: 17253119]

50. Markel MD, Wikenheiser MA, Chao EY. A study of fracture callus material properties: relationship to the torsional strength of bone. J Orthop Res. 1990; 8:843–850. [PubMed: 2213341]

51. Rutten S, Nolte PA, Korstjens CM, et al. Low-intensity pulsed ultrasound increases bone volume, osteoid thickness and mineral apposition rate in the area of fracture healing in patients with a delayed union of the osteotomized fibula. Bone. 2008; 43:348–354. [PubMed: 18538648]

52. Mitsiadis TA, Barrandon O, Rochat A, et al. Stem cell niches in mammals. Exp Cell Res. 2007; 313:3377–3385. [PubMed: 17764674]

53. Wilson A, Trumpp A. Bone-marrow haematopoietic-stem-cell niches. Nature reviews. 2006; 6:93–106.

54. Glennie S, Soeiro I, Dyson PJ, et al. Bone marrow mesenchymal stem cells induce division arrest anergy of activated T cells. Blood. 2005; 105:2821–2827. [PubMed: 15591115]

55. Jung Y, Song J, Shiozawa Y, et al. Hematopoietic stem cells regulate mesenchymal stromal cell induction into osteoblasts thereby participating in the formation of the stem cell niche. Stem Cells. 2008; 26:2042–2051. [PubMed: 18499897]

SUMMARY

In summary, we have determined that transplanted MSC improve the fracture repair process and we have elucidated several of the mechanisms involved in these beneficial effects. We have characterized the dynamic of MSC migration and the essential role of CXCR4, we have found the niches for MSC recruitment at the injury site and we have determined that MSC contribute to the fracture healing by expressing BMP-2 and modulating the injury-related inflammatory response. Our findings provide some critical information to implement the development of MSC-based therapies in patients with poorly healing fractures.

A

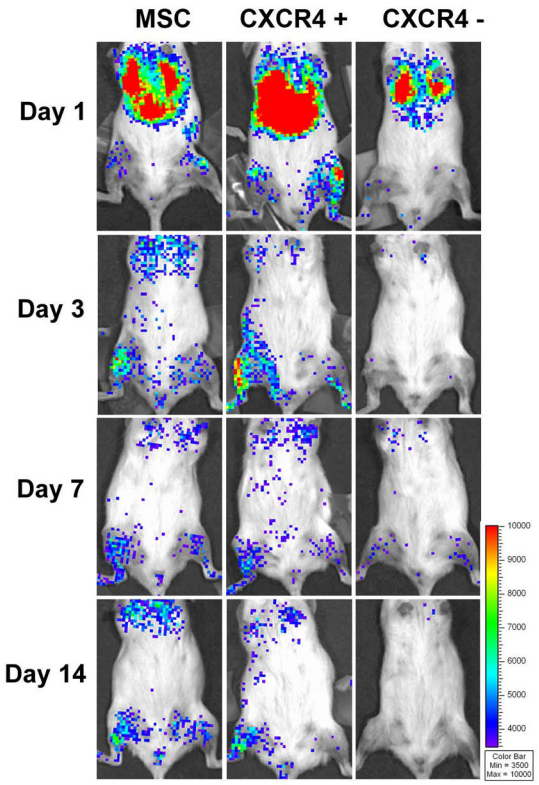

B

	MSC	CXCR4+	CXCR4-	P Value (ANOVA)
Day 3 post-fracture	5317 ± 3468[a] n=14	6464 ± 4814[b] n=8	546 ± 433 n=8	0.0037
Day 7 post-fracture	7093 ± 2041[a] n=6	8526 ± 4202[b] n=4	133 ± 745 n=3	0.0057
Day 14 post-fracture	6508 ± 5350 n=5	18149 ± 6100[a,c] n=3	2440 ± 806 n=3	0.0109

Figure 1. MSC migrate to the fracture site in a time- and CXCR4-dependent manner

(A): BLI was performed at day 1, 3, 7 and 14 after fracture/transplant in mice with tibia fracture transplanted either with 10^6 MSC-β-Act-Luc (MSC) (left panel), MSC-β-Act-Luc-CXCR4+ (CXCR-4+) (middle panel) or MSC-β-Act-Luc-CXCR4-(CXCR-4−) (right panel). Graded color bar indicates BLI signal intensity expressed as photons/sec/cm^2/sr. **(B):** BLI signal semi-quantitative analysis. Signal at the fracture tibia site ROI measured as photons/sec/cm^2/sr, was normalized by subtracting the background signal found in an equal ROI in the contralateral unfractured tibia. [a] $p<0.05$ versus CXCR4-group; [b] $p<0.01$ versus CXCR4-group; [c] $p<0.05$ versus MSC by Tukey post-test. Abbreviations: MSC, mesenchymal stem cells.

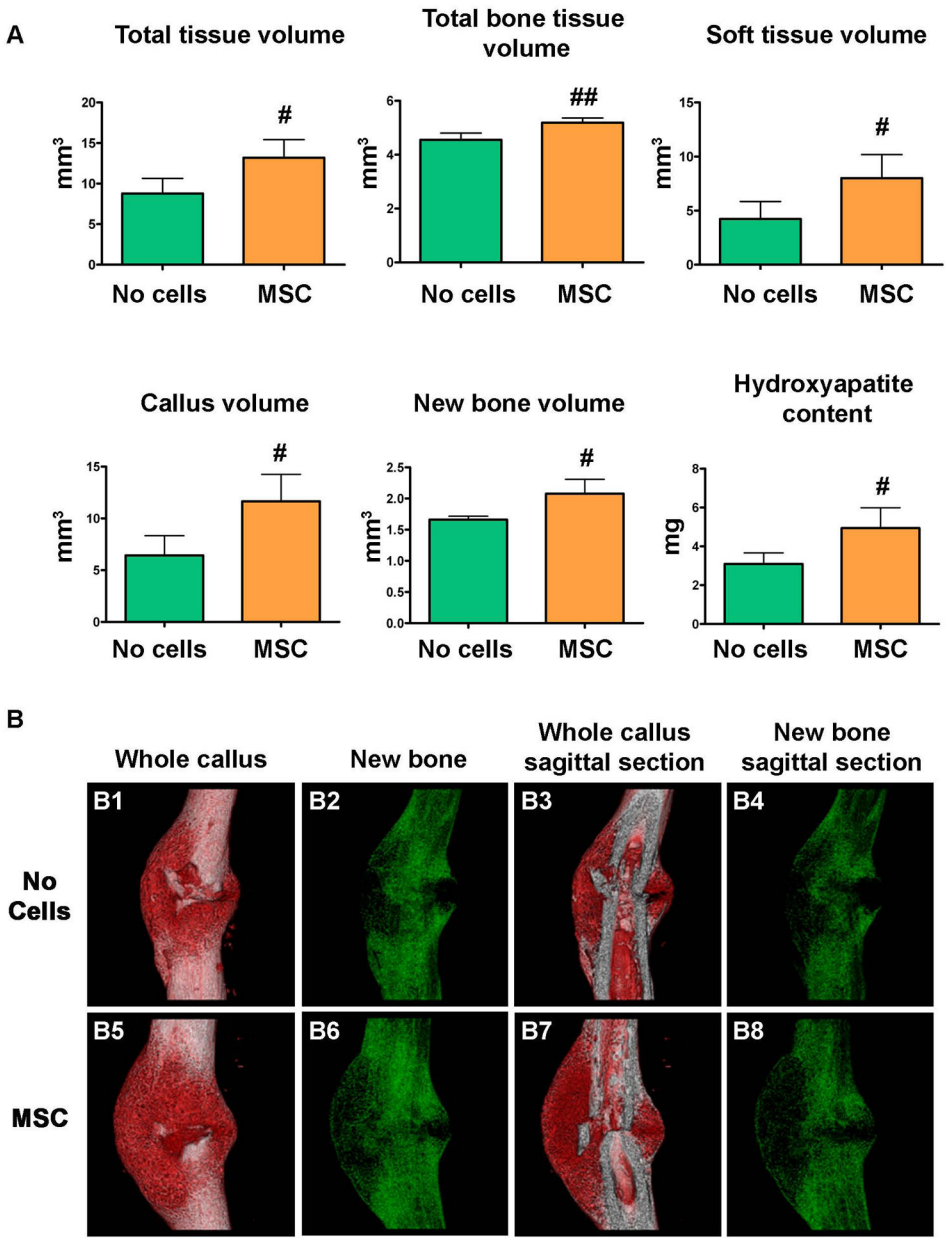

Figure 2. MSC transplant increases callus size and changes callus morphology

(A): μCT analyses were performed 14 days after fracture in calluses dissected from mice that received MSC transplant and controls (no cells). Callus volume and new bone volume were calculated after subtracting the cortical bone volume respectively from the total volume and the total bone tissue volume. #, $p<0.05$ versus No cells; ##, $p<0.01$ versus no cells by Student's *t*-test. No cells, n=3; MSC, n=6.

(B): three-dimensional reconstruction of whole calluses (B1, B2, B5, B6) and sagittal sections (B3, B4, B7, B8) were obtained 14 days after tibial fracture in calluses from mice that were transplanted with MSC or control untransplanted (no cells). Material type analysis of new bone, and soft tissue was determined by a histological-based thresholding of the μCT imaging scans. Abbreviations: MSC, mesenchymal stem cells.

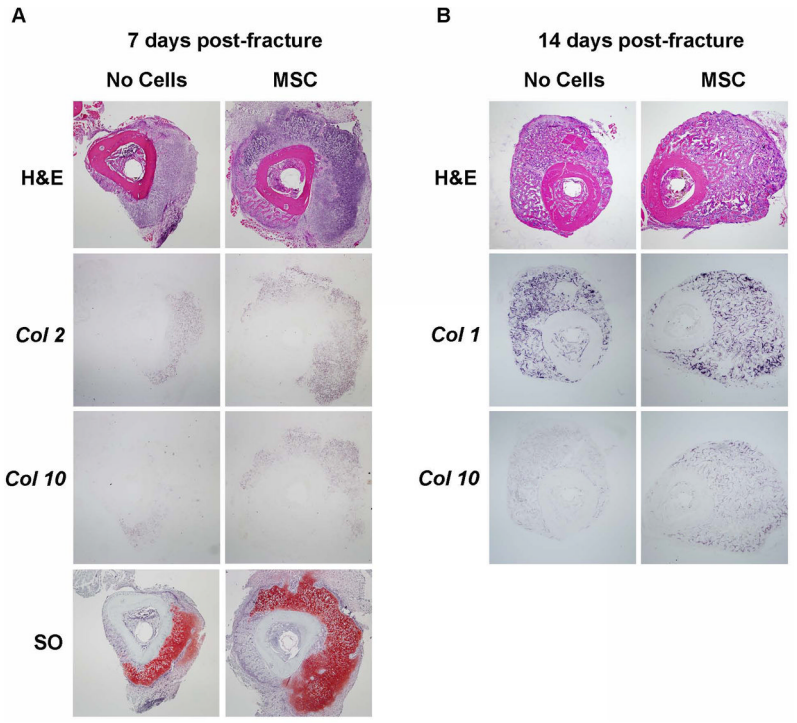

Figure 3. MSC transplant increases the cartilageneous and bone content of the callus

(A): transversal sections of 7 days post-fracture calluses were subjected to H&E and Safranin O staining and *in situ* hybridization for *Collagen-2* and *Collagen-10*. (**B**): 14 days post-fracture transversal sections were subjected to H&E staining and *in situ* hybridization for *Collagen-1* and *Collagen-10*. The entire callus was sectioned (6 μm thick sections), the center of the callus was identified by the largest diameter of callus size by H&E staining and further analyses were performed within 20 sections from the center. Analyses were done in at least 5 sections for each probe or staining. Sections were obtained from at least 3 mice for each group. Abbreviations: H&E, hematoxylin & eosin; Col2, collagen 2; col1, collagen 10; SO, Safranin O; Col1, collagen 1; MSC, mesenchymal stem cells. 40X magnifications are presented.

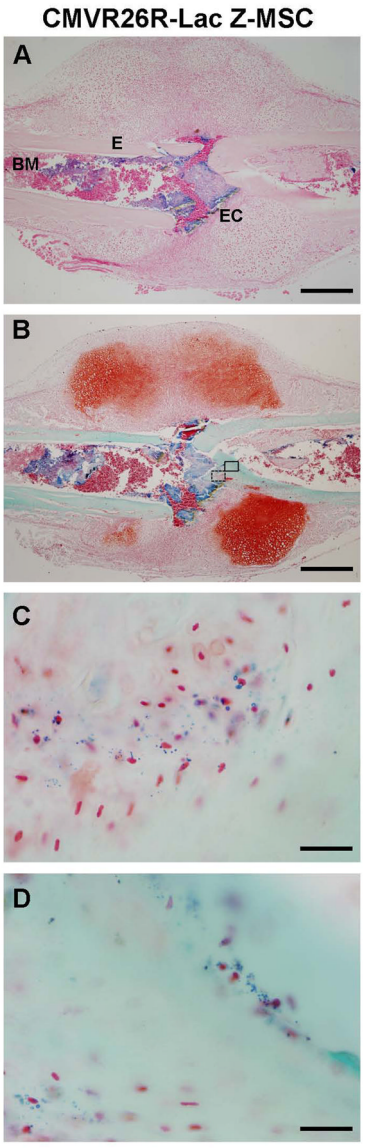

Figure 4. Transplanted MSC localize within specific niches of the fracture callus

10^6 CMVR26-Lac-Z-MSC were transplanted into fractured mice, calluses dissected 7 days after fracture and X-gal stained. **(A):** paraffin sections of the β-gal stained calluses were counter-stained with nuclear Fast Red showing MSC localization into specific areas of the fracture callus. **(B):** paraffin sections of β-gal stained calluses were counter-stained with Safranin O/Fast Green. **(C):** higher magnification of the open box depicted in B, showed MSC embedded into the bone matrix as osteoblasts. **(D):** higher magnification of the close box depicted in B, showed MSC also integrated into the bone matrix as newly formed osteocytes. (**A**, **B**) scale bar 500 micrometers; (**C**, **D**), scale bar 33 micrometers. Sections were obtained from at least 3 mice. Abbreviations: BM, bone marrow (BM); E, endosteum; EC, endosteal callus.

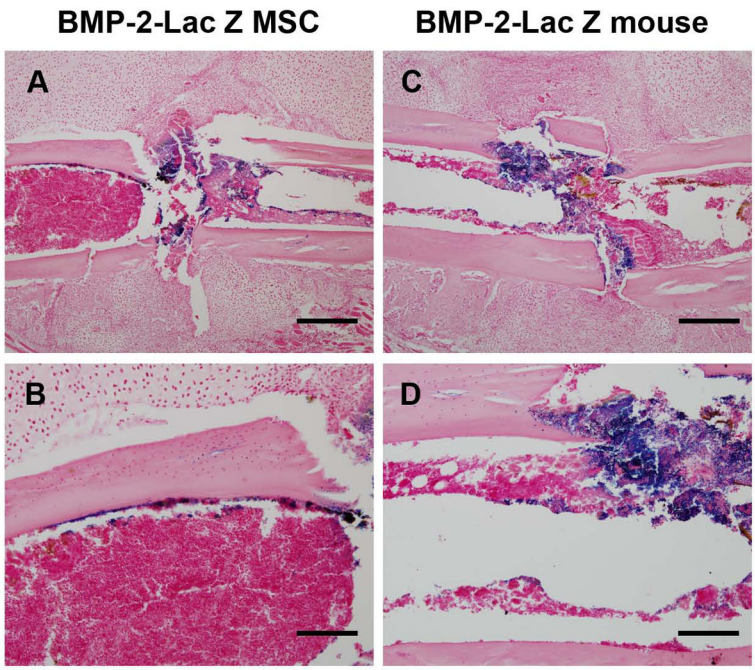

Figure 5. Transplanted MSC express BMP-2 within the fracture and localize at the endosteal site of the callus

(A): 10^6 BMP-2-LacZ-MSC were transplanted into fractured mice and 7 days after fracture the calluses were dissected and X-gal stained. Paraffin sections were counter-stained with nuclear Fast Red showing that MSC localize and express BMP-2 into the fracture rim and endosteum. **(B):** higher magnification of A showing the endosteal localization of MSC expressing BMP-2. **(C):** BMP-2-Lac-Z mice were fractured and 7 days post-fracture calluses were dissected and β-gal stained, paraffin sections were counter-stained with nuclear Fast Red and showed BMP-2 expression at the fracture ridge. **(D):** higher magnification of the fracture rim showing expression of BMP-2. (**A, C)** scale bar 500 micrometers; (**B, D**) scale bar 200 micrometers. Sections were obtained from at least 3 mice. Abbreviations: BMP-2, bone morphogenic protein-2.

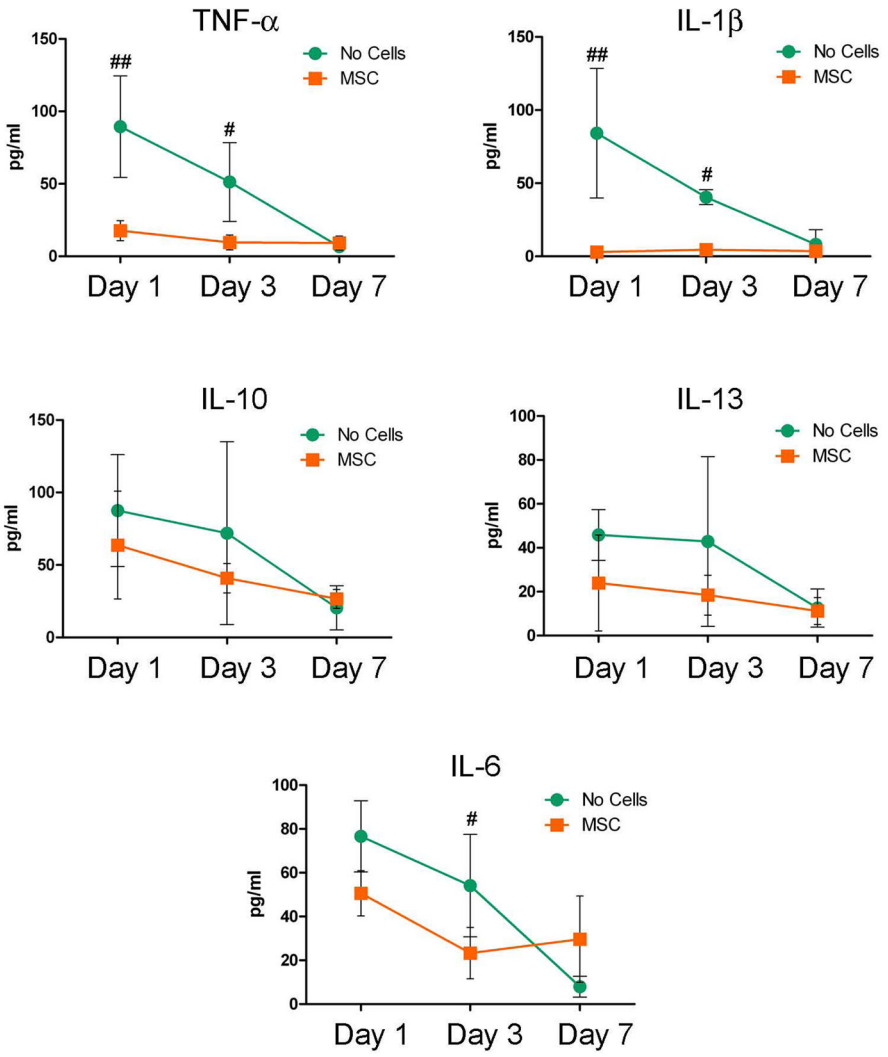

Figure 6. Transplanted MSC have a specific systemic anti-inflammatory effects on the cytokines released after tibia fracture

Cytokines were measured in sera obtained 1, 3 and 7 days after fracture from mice either transplanted with MSC or controls (no cells) by LINCOplex immunoassay. Sera were obtained from at least 4 mice for each group at each corresponding time. #, $p<0.05$ vs control at the corresponding time; ##, $p<0.01$ vs control at the corresponding time by Tukey post-test. Abbreviations: TNF-α, tumor necrosis factor-α; IL-1β, interleukin-1 β, IL-10, interleukin 10; IL-13, interleukin 13; IL-6, interleukin 6.; MSC, mesenchymal stem cells.

Table 1

MSC improve the biomechanical properties of the fracture callus. Fourteen days after tibial fracture, calluses from mice that were transplanted either with MSC or control (no cells) were dissected and subjected to distraction-to-failure BMT.

	No Cells (n=5)	MSC (n=6)
Toughness (N*mm)	0.138 ± 0.044	0.425 ± 0.143[b]
Ultimate Force (N)	1.803 ± 0.488	2.492 ± 0.829
Stiffness (N/mm)	17.790 ± 8.861	12.000 ± 7.591
Ultimate Displacement (mm)	0.124 ± 0.045	0.308 ± 0.148[a]

[a] $p<0.05$ versus No cells;

[b] $p<0.01$ versus No cells by Student's *t*-test.

Abbreviations: MSC, mesenchymal stem cells; BMT, biomechanical testing; N, Newton.